

1 **The spatiotemporal dynamics of recognition memory for complex versus**
2 **simple auditory sequences**

3
4 Fernández Rubio, G.^{1,2*}, Brattico, E.^{1,3}, Kotz, S. A.², Kringelbach, M. L.^{1,4,5}, Vuust, P.¹,
5 Bonetti, L.^{1,4,5}

6
7
8 ¹*Center for Music in the Brain, Department of Clinical Medicine, Aarhus University & The Royal Academy of*
9 *Music, Aarhus, Aalborg, Denmark*

10 ²*Department of Neuropsychology and Psychopharmacology, Faculty of Psychology and Neuroscience,*
11 *Maastricht University, Maastricht, The Netherlands*

12 ³*Department of Education, Psychology, Communication, University of Bari Aldo Moro, Bari, Italy*

13 ⁴*Centre for Eudaimonia and Human Flourishing, University of Oxford, Oxford, United Kingdom*

14 ⁵*Department of Psychiatry, University of Oxford, Oxford, United Kingdom*

15

16

17 *Corresponding author: gemmafr@clin.au.dk

18 ***Abstract***

19 Differently from visual recognition, auditory recognition is a process relying on the
20 organization of single elements that evolve in time. Here, we aimed to discover the
21 spatiotemporal dynamics of this cognitive function by adopting a novel strategy for varying
22 the complexity of musical sequences. We selected traditional tonal musical sequences and
23 altered the distance between pitches to obtain matched atonal sequences. We then recorded
24 the brain activity of 71 participants using magnetoencephalography (MEG) while they
25 listened to and later recognized auditory sequences constructed according to simple (tonal) or
26 complex (atonal) conventions. Results reveal qualitative changes in neural activity dependent
27 on stimulus complexity: recognition of tonal sequences engaged hippocampal and cingulate
28 areas, whereas recognition of atonal sequences mainly activated the auditory processing
29 network. Our findings highlight the involvement of a cortico-subcortical brain network for
30 auditory recognition and support the idea that stimulus complexity qualitatively alters the
31 neural pathways of recognition memory.

32

33 **Keywords**

34 Recognition memory, Stimulus complexity, Predictive coding of music (PCM),
35 Magnetoencephalography (MEG)

36 ***Introduction***

37 Encoding and recognizing sounds that are structurally complex is a cognitive challenge
38 relying on neural mechanisms that are not yet fully elucidated. To memorize complex sound
39 sequences, we likely depend on the temporal organization of a stimulus' components and
40 memory functions ¹.

41 Memory encoding takes place in the hippocampus ²⁻⁴, whereas subsequent processes
42 related to recognition memory are supported by a functional network of interconnected
43 regions in the medial temporal lobe, including the hippocampus, insula, and inferior temporal
44 cortex ^{2, 5, 6}. For memory consolidation, communication between hippocampal and
45 neocortical areas is needed ⁷⁻⁹. Much evidence comes from studies using static visual stimuli,
46 such as pictures of objects, faces, or natural scenes ¹⁰⁻¹². In addition, however, information
47 and meaning unfold over time as the brain attempts to predict upcoming stimuli based on
48 prior memory representations. Hence, to better understand memory recognition and its
49 underlying fast brain dynamics, novel methods must be adopted that highlight the temporal
50 properties of dynamic stimuli. This can be done by studying the neural activity underlying the
51 processing of sound sequences that acquire meaning through their evolution over time, such
52 as music ¹³⁻¹⁵.

53 According to the predictive coding of music (PCM) theory, music processing is bound
54 by hierarchical Bayesian rules, wherein the brain compares musical information with its
55 internal predictive model in an attempt to reduce a prediction error ¹⁶⁻¹⁹. Specifically, bottom-
56 up sensations evoked by auditory stimuli are processed in primary cortices and contrasted
57 with top-down predictions in higher-order cortices to generate musical expectations and
58 minimize hierarchical prediction errors ¹⁹⁻²¹. Predictive mechanisms rely on long- and short-
59 term memory functions, familiarity, and listening strategies to create musical expectations ¹⁸.
60 Overall, the PCM model provides a reliable framework for studying music perception ²²⁻²⁵,
61 training ^{26, 27}, action ^{28, 29}, synchronization ³⁰⁻³², and emotion ³³⁻³⁵. In recent years, studies
62 have also began exploring the neural underpinnings of musical memory. Using functional
63 resonance imaging (fMRI) and a naturalistic music listening paradigm, Alluri et al. ³⁶
64 investigated the neural correlates of music processing and reported activation of cognitive,
65 motor, and limbic brain networks for the continuous processing of timbral, tonal, and
66 rhythmic features. Subsequently, using the same stimuli, Burunat et al. ³⁷ reported the
67 recruitment of memory-related and motor brain regions during the recognition of musical

68 motifs. Despite their contributions, these studies fail to identify the fine-grained temporal
69 mechanisms of sound encoding and memory processes.

70 More recently, we introduced novel applications of magnetoencephalography (MEG)
71 combined with magnetic resonance imaging (MRI) to study music recognition. These studies
72 accentuated the temporal involvement of a widespread cortico-subcortical brain network
73 comprising the primary auditory cortex, superior temporal gyrus, frontal operculum,
74 cingulate gyrus, orbitofrontal cortex, and hippocampus during recognition of auditory
75 (musical) sequences³⁸⁻⁴⁰. Overall, these investigations have provided unique insight into the
76 neural mechanisms underlying the recognition of temporal sequences. What remains to be
77 addressed is how these mechanisms are modulated by stimulus complexity.

78 Here, we used melodic sequences, where meaning emerged from the sequential
79 combination of individual tones over time⁴⁰, and varied the tone distribution to obtain new,
80 complex musical sequences. In this scenario, encoding and recognition of the musical
81 sequences largely depend on the sequential order of the tones that comprise it. We first
82 selected musical sequences based on the rules of tonality, which is the dominant musical
83 system in Western popular music⁴¹. Second, by modifying the tone intervals (i.e., the
84 distances between pitches) while keeping all other variables (e.g., rhythm, tempo, timbre)
85 constant, we generated matched *atonal* musical sequences. The stimulus manipulation was
86 based on previous literature, which reported that tonal rather than atonal musical sequences
87 are overall easier to process⁴²⁻⁴⁶ and more appreciated by non-expert listeners⁴⁶⁻⁴⁸. Unlike
88 tonal music, atonal music is characterized by the absence of a clear tonal center and
89 hierarchical stability, which significantly reduces its predictive value and gives rise to
90 increased prediction errors^{42-45, 49}. Thus, we expected that the alteration of tonal intervals
91 would reduce the predictability of the atonal sequences, leading to increased difficulty to
92 recognize them.

93 To summarize, in the current study we used magnetoencephalography (MEG) and a
94 musical recognition task³⁸⁻⁴⁰ while participants listened to and recognized auditory (musical)
95 sequences of varying complexity. We aimed at describing its fine-grained spatiotemporal
96 dynamics. Following previous studies³⁶⁻⁴⁰, we expected that the recognition of auditory
97 sequences would activate a widespread brain network that includes both auditory (e.g.,
98 primary auditory cortex, superior temporal gyrus, Heschl's gyrus, planum temporale, insula)
99 and memory processing areas (e.g., hippocampus, cingulate gyrus). We further hypothesized
100 that neural activity would be distributed along two main frequency bands that reflected the
101 occurrence of two different cognitive processes: a slow frequency band related to the

102 recognition of the full musical sequence in memory processing areas, and a fast frequency
103 band associated with the processing of each individual tone of the musical sequence in
104 auditory regions. More importantly, we hypothesized that, based on stimulus complexity,
105 tonal music would be more efficiently processed than atonal music, which would be reflected
106 in different behavioral responses and distinct neural pathways during recognition of tonal and
107 atonal sequences.

108 **Results**

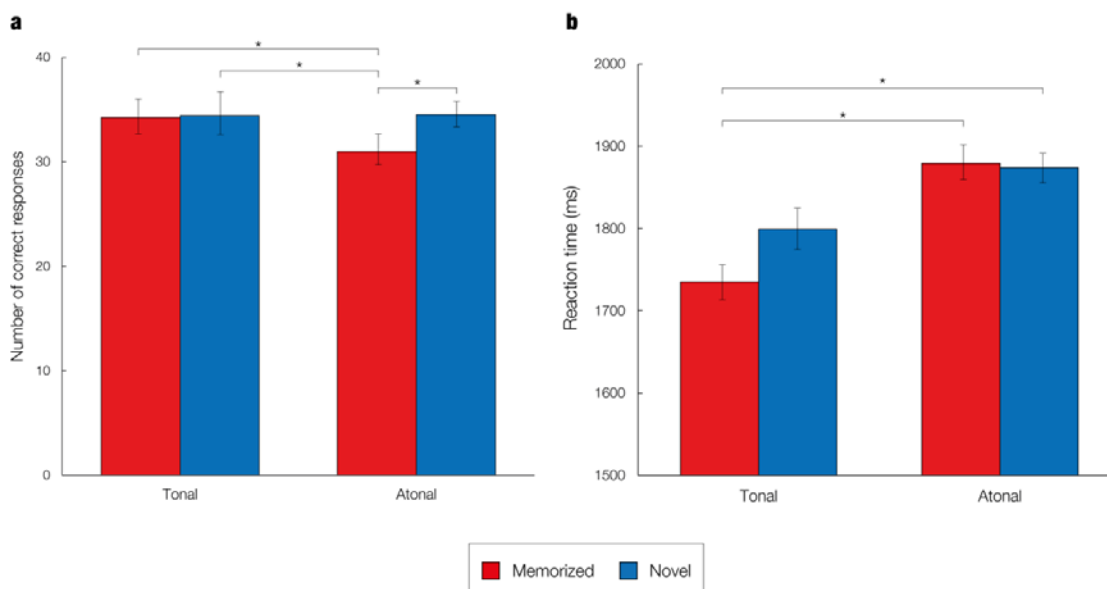
109 **Behavioral data**

110 Participants performed an old/new auditory recognition task. They first listened to a full
111 musical piece (encoding) and subsequently identified which musical sequences were
112 memorized or novel. During recognition, the response accuracy and reaction time of the
113 participants were recorded using a joystick. These behavioral data were statistically analyzed
114 to examine the differences between the four experimental conditions (memorized tonal
115 sequences, novel tonal sequences, memorized atonal sequences, novel atonal sequences).

116 A one-way analysis of variance (ANOVA) showed that the differences in response
117 accuracy were statistically significant, $F(3, 280) = 6.87, p = .002$. Post-hoc analyses indicated
118 that the average number of correct responses was significantly lower for memorized atonal
119 sequences ($M = 30.98, SD = 5.46$) than for novel atonal ($M = 34.51, SD = 4.26, p < .001$),
120 memorized tonal ($M = 34.34, SD = 5.95, p = .002$) and novel tonal sequences ($M = 34.41, SD$
121 $= 6.04, p = .001$). **Figure 2A** shows the average number of correct responses, standard
122 deviation, and statistically significant differences per condition.

123 Regarding the mean reaction time, there was a statistically significant difference between
124 conditions as determined by one-way ANOVA, $F(3, 280) = 4.94, p = .002$. Post-hoc analyses
125 revealed that the average reaction time was significantly lower for memorized tonal
126 sequences ($M = 1735.17, SD = 259.91$) compared to memorized atonal ($M = 1879.44, SD =$
127 $259.34, p = .005$) and novel atonal sequences ($M = 1873.78, SD = 250.48, p = .007$), but not
128 compared to novel tonal sequences ($M = 1799.52, SD = 267.14, p = .450$). **Figure 2B**
129 displays the mean reaction time, standard deviation, and statistically significant differences
130 per condition.

131



132

133 **Figure 2. Analyses of behavioral data**

134 **a** – Average number of correct responses for each of the experimental conditions. Asterisks denote a statistically
135 significant difference between two conditions. Error bars show the standard deviation. **b** – Average reaction
136 times for each of the experimental conditions. Asterisks denote a statistically significant difference between two
137 conditions. Error bars show the standard deviation.

138

139 **MEG sensor data**

140 The MEG data (204 planar gradiometers and 102 magnetometers) were analyzed at the MEG
141 sensor level, using the broadband signal. Although the emphasis of the study lays in
142 identifying the brain areas involved in recognizing tonal versus atonal musical sequences, the
143 MEG sensor data were examined to assess whether the neural signal was significantly
144 different for memorized than for novel trials and thus would corroborate the results
145 of previous studies^{17, 19}.

146 After averaging the epoched data of correct trials for each experimental condition and
147 combining the planar gradiometers, paired-samples t-tests were performed to identify which
148 condition (memorized or novel) generated a stronger neural signal for each time sample and
149 MEG sensor. Cluster-based MCS were then calculated to correct for multiple comparisons.
150 This was performed independently for both tonal and atonal data (see Methods for details).

151 First, paired-samples t-tests ($\alpha = .01$) were calculated for the tonal data in the time
152 interval 0 – 2500 ms (from the onset of the trial) using combined planar gradiometers as these
153 sensors are less affected by external noise than magnetometers⁴²⁻⁴⁵. Next, multiple
154 comparisons were corrected by using cluster-based MCS on the significant t-tests' results (α
155 = .001, 1000 permutations). Three main significant clusters of activity were identified in

156 three specific time intervals when contrasting memorized versus novel sequences, as reported
 157 in **Table 1** and in Supplementary Materials (**Figure SF1** and **Table ST1**). Additionally, two
 158 main significant clusters of activity were detected when contrasting novel versus memorized
 159 sequences (**Table 1**, **Figure SF2**, and **Table ST1**).

160

Cluster number	Size	MEG channels	Time interval (seconds)	<i>p</i> -value
<i>Memorized versus novel tonal sequences</i>				
1	224	63	0.14 – 0.187	<.001
2	180	29	0.987 – 1.153	<.001
3	150	37	0.807 – 0.887	<.001
<i>Novel versus memorized tonal sequences</i>				
1	277	36	0.64 – 0.8	<.001
2	242	30	0.38 – 0.513	<.001

161

162 **Table 1**

163 Significant clusters of activity for the tonal MEG sensor data.

164

165 Regarding the atonal data, paired-samples t-tests ($\alpha = .01$) were calculated in the same
 166 time interval (0 – 2500 ms) using combined planar gradiometers. Next, multiple comparisons
 167 were corrected for by using MCS on the significant t-tests' results ($\alpha = .001$, 1000
 168 permutations). This procedure identified three main significant clusters of activation when
 169 contrasting memorized versus novel excerpts (**Table 2**, **Figure SF3**, and **Table ST1**). In the
 170 case of the novel versus memorized contrast, three main significant clusters of activity were
 171 found (**Table 2**, **Figure SF4**, and **Table ST1**).

172

Cluster number	Size	Channels	Time interval (seconds)	<i>p</i> -value
<i>Memorized versus novel atonal sequences</i>				
1	288	40	0.68 – 0.9	<.001
2	215	44	0.52 – 0.66	<.001
3	135	40	0.133 – 0.187	<.001
<i>Novel versus memorized atonal sequences</i>				
1	478	52	1.167 – 1.267	<.001
2	345	42	0.893 – 0.987	<.001
3	320	44	0.653 – 0.74	<.001

173

174 **Table 2**

175 Significant clusters of activity for the tonal MEG sensor data.

176

177 **Source reconstruction**

178 After examining the strength of the neural signals at the MEG sensor level, we focused on the
179 main aim of the study, namely to investigate the neural differences underlying the recognition
180 of tonal versus atonal musical sequences in MEG reconstructed source space. To perform this
181 analysis, we localized the brain sources of the neural signal recorded by the MEG channels.
182 This was performed for both the tonal and atonal data and for two frequency bands (delta [0.1
183 – 1 Hz] and theta [2 – 8 Hz]) that were previously described by Bonetti et al.^{38, 40} and
184 presumably linked to the processing of the single components (theta) relative to the wholistic
185 sequence (delta).

186

187 *Delta band (0.1 – 1 Hz)*

188 The neural sources were calculated using a beamformer approach. First, a forward model was
189 computed by considering each brain source as an active dipole and calculating its strength
190 across the MEG sensors. Second, a beamforming algorithm was used as an inverse model to
191 estimate the brain sources of the neural activity based on the MEG recordings.

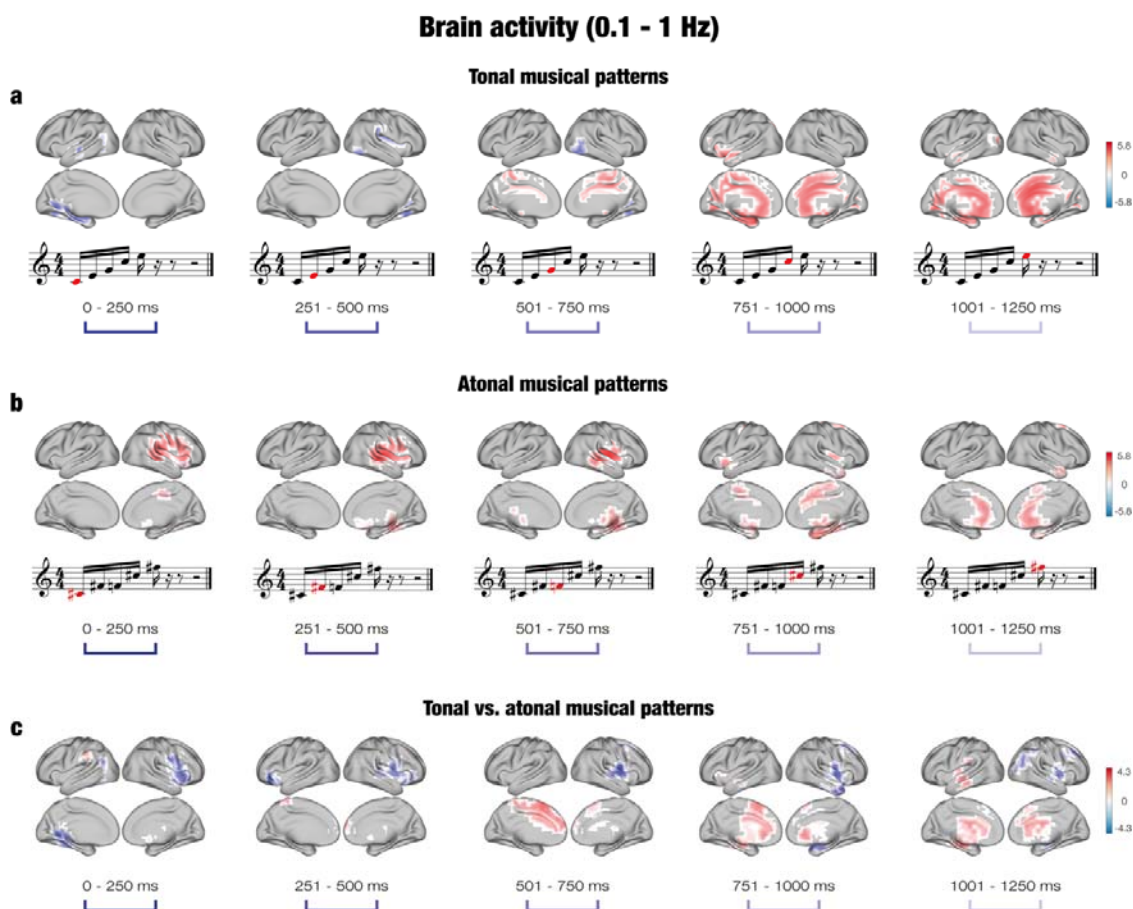
192 After computing the neural sources, a GLM was calculated at each timepoint and dipole
193 location. A series of t-tests ($\alpha = .05$) was carried out at the first and group level to estimate
194 the main effect of memorized and novel conditions and their contrast for both the tonal and
195 atonal data independently. Cluster-based MCS ($\alpha = .001$, 1000 permutations) were computed
196 to correct for multiple comparisons and to determine the brain activity underlying the
197 development of the musical sequences. These analyses were carried out for five specific time
198 intervals that corresponded to each of the tones comprising the sequences: first tone (0 – 250
199 ms), second tone (251 – 500 ms), third tone (501 – 750 ms), fourth tone (751 – 1000 ms), and
200 fifth tone (1001 – 1250 ms). This was estimated for the memorized versus novel contrast for
201 both tonal and atonal sequences independently and for memorized tonal versus memorized
202 atonal sequences.

203 Significant clusters of activity ($p < .001$) were located across a number of brain voxels
204 (k) for each tone of the tonal sequences, as reported in **Table ST2**. For memorized tonal
205 sequences, the neural activity was overall stronger for the third ($k = 69$), fourth ($k = 266$), and
206 fifth tones ($k = 229$). The largest differences were localized in the middle cingulate gyrus,

207 right supplementary motor area, precuneus, and left lingual gyrus for the third tone; the left
208 amygdala, left parahippocampal gyrus, left lingual gyrus, left hippocampus, and middle
209 cingulate gyrus for the fourth tone, and the anterior and middle cingulate gyrus and left
210 lingual gyrus for the last tone. For novel tonal sequences, the brain activity was stronger
211 for the first ($k = 54$) and second tones ($k = 29$). In particular, the difference between novel
212 and memorized sequences was strongest in the left calcarine fissure, left lingual gyrus, left
213 hippocampus, left precuneus, and left superior temporal gyrus for the first tone, and the right
214 fusiform gyrus, right lingual gyrus, and right inferior occipital gyrus for the second tone. The
215 contrast between memorized and novel tonal sequences for the delta band is depicted in
216 **Figure 3A**.

217

218



219

220

221 **Figure 3. Brain activity underlying the recognition of musical sequences at the delta band (0.1 – 1**
222 **Hz)**

223 **a** – For tonal sequences, the brain activity was stronger for memorized than novel sequences, particularly for the
224 third (501 – 750 ms), fourth (751 – 1000 ms), and fifth (1001 – 1250) tones. The difference was localized in
225 memory processing areas such as the cingulate gyrus, hippocampus, and parahippocampal gyrus. **b** – For atonal
226 sequences, the brain activity was stronger for memorized than novel sequences for all tones. The difference was
227 mainly localized in auditory processing areas (e.g., superior temporal gyrus, Heschl’s gyrus) for the first three
228 tones, and in memory processing areas (e.g., parahippocampal gyrus, hippocampus) for the fourth and fifth
229 tones. **c** – For the contrast between tonal and atonal sequences, the brain activity was localized in memory
230 processing areas for tonal sequences, particularly for the last three tones, and in auditory processing areas for
231 atonal sequences for all tones.

232

233 In the case of atonal sequences, significant clusters of activity were located for
234 memorized sequences primarily in the right hemisphere, and the neural activity was stronger
235 for memorized than novel sequences across all five tones ($k_1 = 132$, $k_2 = 163$, $k_3 = 130$, $k_4 =$
236 140 , $k_5 = 64$), as reported in **Table ST2**. In particular, the brain activity was strongest in the
237 right Rolandic operculum, right superior temporal gyrus, right Heschl’s gyrus, right
238 supramarginal gyrus, and right insula for the first tone; the right Heschl’s gyrus, right
239 superior temporal gyrus, right Rolandic operculum, right middle temporal gyrus, and right
240 insula for the second tone; the right putamen, right insula, right Rolandic operculum, right
241 Heschl’s gyrus, and right thalamus for the third tone; the parahippocampal gyrus, right
242 fusiform gyrus, right hippocampus, and putamen for the fourth tone; and the anterior
243 cingulate cortex, middle frontal gyrus, and caudate nucleus for the last tone. No significant
244 clusters of activity were located in the delta band for novel atonal sequences. **Figure 3B**
245 pictures the contrast between memorized and novel atonal sequences in the delta band.

246 Regarding the contrast between memorized tonal and atonal sequences, significant
247 clusters of activity were located for both types of musical sequences across all tones (see
248 **Table ST2**). For tonal sequences, the number of significant voxels was higher for the third (k
249 $= 70$) and fifth tones ($k = 79$), whereas for atonal sequences the number of significant brain
250 voxels was higher for the first ($k = 98$), second ($k = 80$), and fourth tones ($k = 103$). In the
251 case of memorized tonal sequences, the neural activity was localized in the the supplementary
252 motor area, left median cingulate gyrus, and superior frontal gyrus for the third tone, and the
253 left hippocampus, left superior temporal gyrus, left thalamus, left insula, left putamen, and
254 left parahippocampal gyrus for the fifth tone. For memorized atonal sequences, the neural
255 activity was localized in the left lingual gyrus, left precuneus, left calcarine fissure, middle
256 temporal gyrus, and right insula at the first tone; the inferior frontal gyrus, right precentral
257 gyrus, right Rolandic operculum, and right superior temporal gyrus for the second tone; the

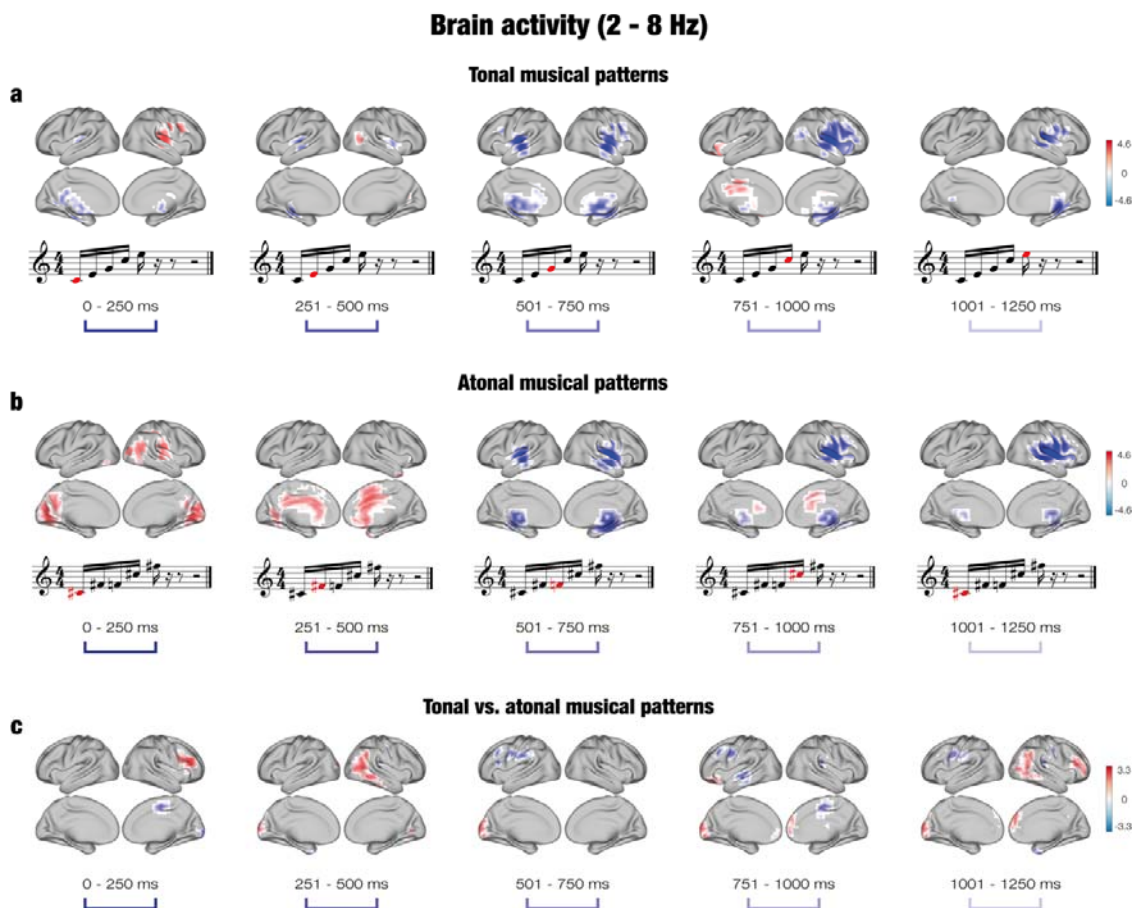
258 right Rolandic operculum, right middle frontal gyrus, right postcentral gyrus, right putamen,
259 and right insula for the fourth tone; and the right middle frontal gyrus, right angular gyrus,
260 and right thalamus for the last tone. The contrast between memorized tonal and atonal
261 sequences in the delta band is shown in **Figure 3C**.

262

263 *Theta band (2 – 8 Hz)*

264 The same procedure was carried out for assessing the brain activity underlying the
265 recognition of musical sequences in the fast frequency band (2 – 8 Hz). Once the GLM was
266 computed, cluster-based MCS ($\alpha = .001$, 1000 permutations) were calculated for five time
267 intervals corresponding to each of the five tones that formed the sequence. Again, this was
268 estimated for the memorized versus novel contrast for both tonal and atonal sequences
269 and memorized tonal versus memorized atonal sequences.

270 Regarding the contrast for tonal sequences, significant clusters of activity ($p < .001$)
271 were located in multiple brain voxels for both memorized and novel sequences, as reported in
272 **Table ST2**. For memorized tonal sequences, the neural activity was overall stronger for the
273 first tone ($k = 74$), whereas it was stronger for novel tonal sequences for the second ($k = 36$),
274 third ($k = 200$), fourth ($k = 196$), and fifth tones ($k = 70$). The brain activity was localized in
275 the right Rolandic operculum, right insula, right Heschl's gyrus, and right superior temporal
276 gyrus for the first tone for memorized tonal sequences. For novel tonal sequences, the main
277 active areas were the left superior temporal gyrus, insula, Heschl's gyrus, and left
278 hippocampus for the second tone; Heschl's gyrus, superior temporal gyrus, insula, and
279 putamen ($k = 11$) for the third tone; right Heschl's gyrus, right insula, right Rolandic
280 operculum, and right superior temporal gyrus for the fourth tone; and the right Rolandic
281 operculum, right Heschl's gyrus, right hippocampus, and right thalamus for the fifth tone.
282 **Figure 4A** displays the contrast between memorized and novel tonal sequences.



283

284

285 **Figure 4. Brain activity underlying the recognition of musical sequences at the theta band (2 – 8**
 286 **Hz)**

287 **a** – For tonal sequences, the brain activity was stronger for novel than memorized sequences, particularly for the
 288 last three tones. The difference was localized in auditory processing areas such as Heschl’s gyrus, superior
 289 temporal gyrus, and Rolandic operculum. The brain activity was stronger for memorized than novel sequences
 290 for the first, second and fourth tones in areas such as the Rolandic operculum (tone 1), occipital gyrus (tone 2)
 291 and inferior frontal gyrus (tone 4). **b** – For atonal sequences, the brain activity was stronger for novel than
 292 memorized sequences for the last three tones in areas such as the insula, Heschl’s gyrus, and superior temporal
 293 gyrus. The brain activity was stronger for memorized than novel sequences for the first two tones in the
 294 calcarine fissure and cingulate gyrus. **c** – For the contrast between tonal and atonal sequences, the brain activity
 295 was mostly scattered and weak, but the neural activity was stronger in the frontal gyrus (tones 1, 4, and 5),
 296 temporal gyrus (tones 2 and 3), and occipital gyrus (tones 2 – 5) for tonal memorized sequences, and in the
 297 supplementary motor area (tone 1), frontal gyrus (tones 3 and 4), middle temporal gyrus (tone 4) and postcentral
 298 gyrus (tone 5) for atonal memorized sequences.

299

300 For the contrast between memorized and novel atonal sequences, the majority of
 301 significant clusters of activity were localized for the first ($k = 166$) and second tones ($k = 104$)

302 for memorized sequences, and for the third ($k = 189$), fourth ($k = 118$), and fifth tones ($k =$
303 156) for novel sequences, as reported in **Table ST2**. For memorized atonal sequences, the
304 neural activity was strongest at the calcarine fissure, lingual gyrus, and right Rolandic
305 operculum for the first tone, and the cingulate gyrus, right supplementary motor area, and
306 superior frontal gyrus for the second tone. For novel atonal sequences, the neural activity was
307 strongest at the insula, putamen, superior temporal gyrus, and Heschl's gyrus for the third
308 tone; the right insula, right putamen, right Heschl's gyrus, right Rolandic operculum, and
309 right superior temporal gyrus for the fourth tone; and the right insula, right Rolandic
310 operculum, right Heschl's gyrus, right putamen, and right superior temporal gyrus for the
311 fifth tone. The contrast between memorized and novel atonal sequences for the theta band is
312 shown in **Figure 4B**.

313 Finally, the significant clusters of activity in the tonal versus atonal contrast for the theta
314 band are reported in **Table ST2**. In the case of memorized tonal sequences, the number of
315 significant brain voxels was higher for the first ($k = 20$), second ($k = 44$), fourth ($k = 45$), and
316 fifth tones ($k = 71$). The neural activity was located in the right inferior frontal gyrus and right
317 middle frontal gyrus for the first tone; the right middle temporal gyrus, right inferior parietal
318 gyrus, right angular gyrus, middle occipital gyrus, and left superior occipital gyrus for the
319 second tone; the frontal gyrus for the fourth tone; and the right middle occipital gyrus, right
320 frontal gyrus, and right middle temporal gyrus for the fifth tone. For memorized atonal
321 sequences, the number of significant voxels was higher for the third tone ($k = 38$) and the
322 neural activity was mainly localized in the left inferior frontal gyrus, left middle frontal
323 gyrus, left supramarginal gyrus, and right supplementary motor area. **Figure 4C** shows the
324 contrast between tonal and atonal sequences for the theta band.

325 Altogether, we found significant differences between tonal and atonal sequences,
326 especially for the slow frequency band. Recognition of memorized tonal sequences elicited
327 stronger neural activity in left cingulate and hippocampal areas in the last three tones of the
328 sequences, whereas recognition of memorized atonal sequences was supported by activation
329 in right auditory regions from the second tone onwards.

330 ***Discussion***

331 This study set out to investigate the brain activation underlying the recognition of auditory
332 musical sequences characterized by different levels of complexity (tonal and atonal).
333 Behavioral data showed clear differences between the recognition of tonal and atonal
334 sequences and significant clusters of activation were observed at the MEG sensor level.
335 Source reconstruction analyses indicated different activation clusters for tonal and atonal
336 sequences, particularly in the delta frequency band. Overall, the neural activity was stronger
337 in memory processing areas for memorized tonal sequences and in auditory processing
338 regions for memorized atonal sequences.

339 Prior to focusing on the differences in brain activity related to distinct levels of
340 recognition complexity, we verified that the current results were consistent with previous
341 studies. Indeed, the brain areas activated during the recognition of tonal sequences confirmed
342 the involvement of a widespread brain network including both auditory and memory
343 processing regions^{36-38, 40}. Furthermore, in accordance with previous research, the neural
344 activity was clearly distributed in two frequency bands^{38, 39}. Delta band (0.1 – 1 Hz) was
345 linked to the recognition of the whole auditory sequences (*global processing*), which was
346 reflected by the stronger activation occurring in this band for the recognition of the
347 memorized sequences. Conversely, theta band (2 – 8 Hz) was associated with the processing
348 of the individual tones (*local processing*), as suggested by the stronger neural activity in
349 auditory regions during processing of novel sequences.

350 Regarding the recognition of tonal and atonal sequences, we observed distinct neural
351 pathways when processing and recognizing the two types of auditory stimuli. While the
352 recognition of tonal sequences mainly recruited a widespread brain network involving
353 cingulate gyrus and hippocampus in the right hemisphere, the recognition of atonal sequences
354 was mainly associated with a sustained, slow activity in the left auditory cortex. These results
355 can be interpreted in light of different theoretical frameworks, namely predictive coding,
356 harmonicity, and global neuronal workspace (GNW). According to PCM theory, the brain's
357 predictive model is being continuously updated while listening to music in order to decrease
358 precision-weighted prediction errors^{16, 18, 19}. The predictive value of atonal music is weaker
359 than tonal music, which alters its complexity and increases prediction errors^{42-46, 49}. In turn,
360 this change in stimulus predictability undermines the processing⁴²⁻⁴⁶ and enjoyment⁴⁶⁻⁴⁸ of
361 atonal music. This was apparent when examining the behavioral results, since memorized
362 atonal sequences were more slowly and less accurately recognized. In addition, the

363 distribution of the neural activity in two frequency bands suggests a combination of top-down
364 predictions in the delta band, which is related to the recognition of memorized sequences, and
365 bottom-up predictions in the theta band, as the prediction error increases with novel
366 sequences.

367 An alternative explanation for these results focuses on the harmonicity of auditory
368 stimuli. Tonal music has been closely linked to the harmonic series, a natural sequence of
369 sound frequencies that are integer multiples of a fundamental. Environmental sounds are
370 typically nonharmonic, whereas both human and animal vocalizations contain harmonic
371 structures⁶³. The tonotopic organization of the human auditory cortex is particularly sensitive
372 to harmonic tones, suggesting that this region developed to process harmonics due to their
373 relevance for social communication^{64, 65}. These results indicate that distinct neural pathways
374 are activated when recognizing auditory stimuli that are not coherent with the natural
375 harmonic series and thus arguably more complex to process. Indeed, we found that for
376 memorized tonal sequences, the brain activity was primarily located at the cortico-
377 hippocampal network in the right hemisphere, and for memorized atonal sequences the
378 auditory network in the left hemisphere. Specifically, the strong activation in low-processing
379 primary auditory regions at the first three tones of the atonal sequences suggests a
380 “disentangling” of the sequence before it can be processed and recognized by high-cognitive
381 areas involved in memory processing. One possible approach to further test the harmonicity
382 hypothesis in relation to sequence recognition would be to create a collection of pieces that
383 are systematically varied in terms of their similarity to the natural harmonic series. Future
384 studies are called to investigate such perspectives.

385 Finally, the current results are also consistent with the GNW hypothesis^{66, 67}. According
386 to this theory, stimuli become conscious when they ignite late, high-order regions in response
387 to the activation of sensory cortices involved in perceptual representation. Conversely,
388 unconscious information does not reach high-processing brain areas and neural activity is
389 limited to sensory cortices^{66, 68, 69}. Importantly, we found that tonal sequences induced a late
390 and robust activation of memory processing regions. Although it is unclear *why* atonal
391 sequences were differently processed by the brain, we can confirm that the complexity of the
392 stimuli modulates the transition from primary sensory areas to the GNW, adding new
393 information to this comprehensive theoretical framework.

394 The current study provides valuable insights into the brain mechanisms underlying the
395 recognition of auditory sequences. The results are consistent with those of previous studies
396 and evidence of the engagement of a large brain network that comprises both memory

397 processing and auditory regions when recognizing music. Results further highlight the
398 importance of stimulus complexity for the processing of temporal sequences and hint that the
399 brain employs different strategies to account for this complexity.

400 **Acknowledgements**

401 We thank Giulia Donati, Riccardo Proietti, Giulio Carraturo, Mick Holt, Holger Friis for
402 their assistance in the neuroscientific experiment.

403 The Center for Music in the Brain (MIB) is funded by the Danish National Research
404 Foundation (project number DNRF117). Additionally, we thank the Fundación Mutua
405 Madrileña for the economic support provided to the author GFR and the University of
406 Bologna for the economic support provided to student assistants Giulia Donati, Riccardo
407 Proietti and Giulio Carraturo.

408 LB is supported by Carlsberg Foundation (CF20-0239), Center for Music in the Brain,
409 Linacre College of the University of Oxford, and Society for Education and Music
410 Psychology (SEMPRE's 50th Anniversary Awards Scheme).

411 MLK is supported by Center for Music in the Brain and Centre for Eudaimonia and
412 Human Flourishing, which is funded by the Pettit and Carlsberg Foundations.

413 **Author contributions**

414 LB, EB, MLK, and PV conceived the hypotheses, designed the study, and recruited the
415 resources for the experiment. LB and GFR performed pre-processing and statistical
416 analysis. EB, SAK, LB, MLK, and PV provided essential help to interpret and frame the
417 results within the neuroscientific literature. GFR and LB wrote the first draft of the
418 manuscript and prepared the figures. All the authors contributed to and approved the final
419 version of the manuscript.

420 **Competing interests' statement**

421 The authors declare no competing interests.

422 *Materials and methods*

423 **Participants**

424 The participant sample consisted of 71 volunteers (38 males and 33 females) aged 18 to 42
425 years old (mean age: 25 ± 4.10 years). All participants were healthy and reported normal
426 hearing. Participants were recruited in Denmark and came from Western countries with
427 matching socioeconomic and educational backgrounds.

428 The project was approved by the Ethics Committee of the Central Denmark Region (De
429 Videnskabetiske Komitéer for Region Midtjylland, Ref 1-10-72-411-17). The experimental
430 procedures were carried out in compliance with the Declaration of Helsinki – Ethical
431 Principles for Medical Research. All participants gave the informed consent before starting
432 the experimental procedure.

433

434 **Experimental stimuli and design**

435 Two musical compositions were used in the experiment: the right-hand part of Johann
436 Sebastian Bach's Prelude No. 1 in C Major, BWV 846 (hereafter referred to as the “tonal
437 piece”), and an atonal version of the prelude (hereafter referred to as the “atonal piece”).
438 MIDI versions were created using Finale (MakeMusic, Boulder, CO) and both pieces lasted
439 2.5 minutes each, with the same duration for all tones. LB composed the atonal piece based
440 on the tonal piece. In particular, new tones were assigned to each of the tones comprising
441 Bach's original prelude. These new tones were one or two semitones higher or lower than the
442 original tones, and the same tone conversion was applied throughout the entire tonal piece to
443 obtain the atonal piece (e.g., every C tone in the tonal piece was converted into a C sharp in
444 the atonal piece). Thus, both compositions were identical in terms of the sequential
445 presentation of the tones (i.e., if C was positioned as 1st, 7th, and 8th tone in the tonal piece, C
446 sharp occupied the same positions [1st, 7th, and 8th] in the atonal piece), their rhythmic
447 pattern, dynamics, and duration. Thus, the crucial difference between the two pieces was that
448 the tonal piece was in the key of C Major, whereas the atonal piece did not have a musical
449 key. The first two bars of each piece are displayed in **Figure 1a**, showing similarities and
450 correspondence between the two pieces.

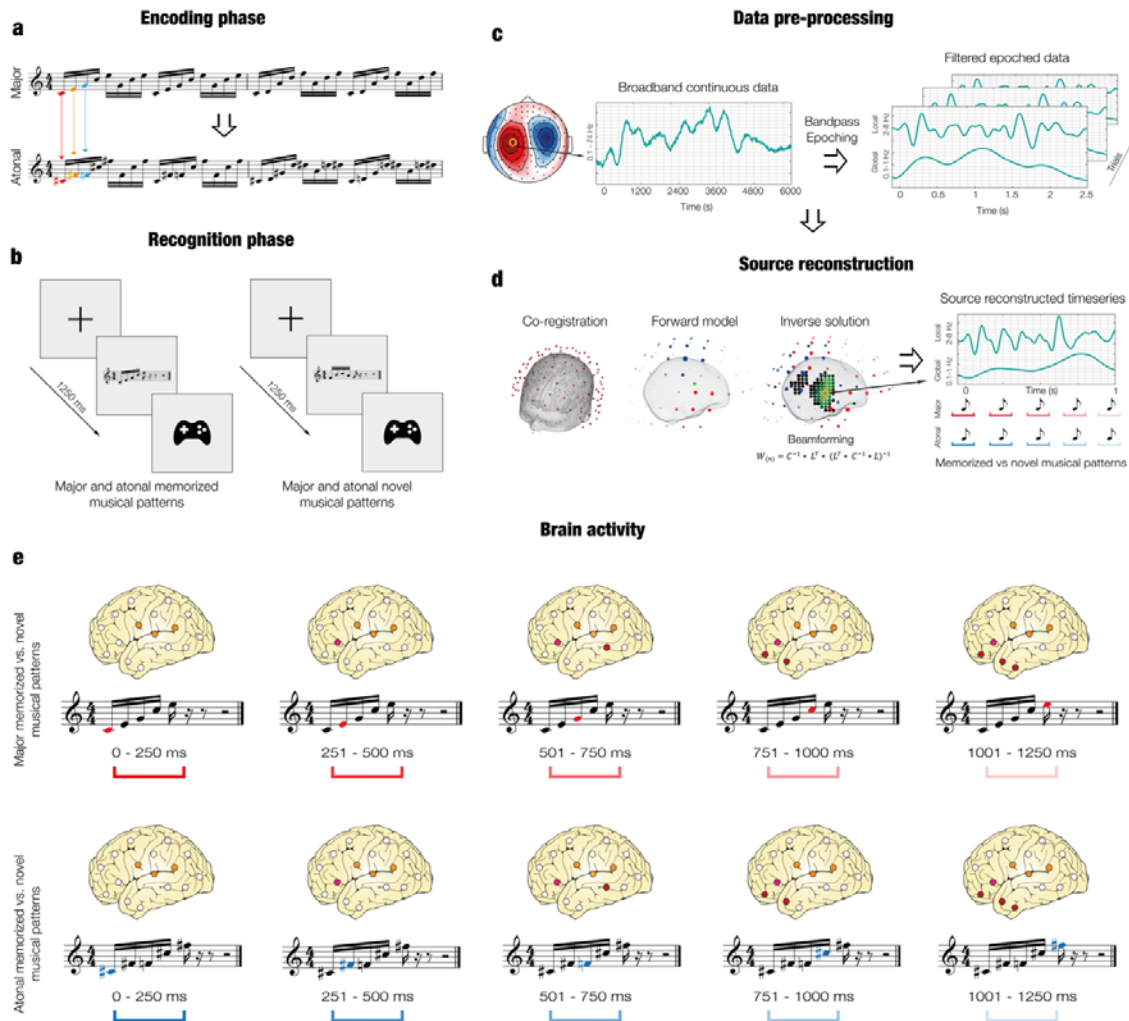
451 Forty musical excerpts (i.e., short melodies or sequences) were extracted from each of
452 the pieces. All excerpts consisted of the first five notes of each bar and lasted for 1250 ms
453 (250 ms per note). In addition, 40 new excerpts were created for each piece based on the
454 original ones. These new sequences were matched to the original ones among several

455 variables, to prevent potential confounds. Specifically, they were matched for rhythm,
456 volume, timbre, tempo, meter, and tonality.

457 The stimuli were employed in an old/new auditory recognition paradigm, as depicted in
458 **Figure 1b**, that was administered to the participants while their brain activity was recorded
459 using MEG. The paradigm consisted of two parts, encoding and recognition, and was
460 performed twice, once for the tonal piece and once for the atonal piece. The order of
461 tonal/atonal was counterbalanced across participants. During the encoding part, participants
462 actively listened to four repetitions of the entire musical piece (tonal or atonal) and tried to
463 memorize it as much as possible. Afterwards, they were presented with the previously
464 described 80 musical excerpts (40 memorized and 40 novel excerpts, randomly ordered) and
465 stated whether the excerpts belonged to the piece they had previously listened to
466 (“memorized”) or whether they were new excerpts (“novel”). Response accuracy and reaction
467 time were recorded using a joystick.

468

469



470

471

472 **Figure 1. Experimental stimuli and design, data analyses and (temporal) brain activity**

473 **a** – Two musical pieces were used in the experiment: the right-hand part of J. S. Bach’s Prelude No. 1 in C
 474 Major, BWV 846 (i.e., “tonal”, top row), and an atonal version of the prelude (i.e., “atonal”, bottom row). Both
 475 pieces were matched in terms of the sequential presentation of the tones, rhythmic patterns, dynamics, and
 476 duration, and their melodic contour was almost identical. The atonal piece was created by LB by assigning new
 477 tones that were one or two semitones lower or higher than the original tones of the tonal piece. For example, C
 478 (in red) was converted into C sharp (in red), E (in orange) was converted into F sharp (in orange), G (in blue)
 479 was converted into F (in blue), etc. **b** – Participants performed the experimental task twice (once for the tonal
 480 piece and once for the atonal piece) and the order of presentation was randomized across participants. After
 481 listening to the full piece, participants were presented with excerpts that belonged to the piece or with new
 482 excerpts and were asked to state whether the excerpts were “memorized” or “novel” using a joystick. **c** – The
 483 task was administered to the participants while their brain activity was recorded using MEG. The continuous
 484 neural data was preprocessed. **d** – Source reconstruction analyses were conducted to identify the brain sources
 485 that generated the neural activity. The data was first bandpass-filtered into two frequency bands (0.1 – 1 Hz and
 486 2 – 8 Hz) and the MEG and MRI data were co-registered. An overlapping-spheres forward model was computed

487 using an 8-mm grid and a beamforming algorithm was applied as the inverse solution. Finally, the source
488 reconstructed time series was computed for both tonal and atonal data and their contrast in both frequency
489 bands. e – Contrasts between memorized and novel sequences were calculated for each tone that comprised the
490 tonal and atonal musical sequences for both frequency bands.

491

492 **Data acquisition**

493 The MEG recordings were acquired in a magnetically shielded room at Aarhus University
494 Hospital (Denmark) with an Elekta Neuromag TRIUX MEG scanner with 306 channels
495 (Elekta Neuromag, Helsinki, Finland). The data were recorded at a sampling rate of 1000 Hz
496 with an analogue filtering of 0.1 – 330 Hz. Before starting the recordings, the head shape of
497 the participants and the position of four Head Position Indicator (HPI) coils with respect to
498 three anatomical landmarks were registered using a 3D digitizer (Polhemus Fastrak,
499 Colchester, VT, USA). This information was later used to co-register the MEG data with the
500 MRI anatomical scans. During the MEG recordings, the HPI coils registered the continuous
501 head localization, which was subsequently used for movement correction analyses.
502 Additionally, two sets of bipolar electrodes were used to record eye movements and cardiac
503 rhythm for later removing electrooculography (EOG) and electrocardiography (ECG)
504 artifacts.

505 The MRI scans were recorded on a CE-approved 3T Siemens MRI-scanner at Aarhus
506 University Hospital (Denmark). The data were recorded using a structural T1 with a spatial
507 resolution of 1.0 x 1.0 x 1.0 mm and the following sequence parameters: echo time (TE) =
508 2.96 ms, repetition time (TR) = 5000 ms, reconstructed matrix size = 256 x 256, bandwidth =
509 240 Hz/Px.

510 The MEG and MRI recordings were acquired in two separate sessions.

511

512 **Data preprocessing**

513 The raw MEG sensor data (204 planar gradiometers and 102 magnetometers) were first
514 preprocessed by MaxFilter⁵⁰ in order to suppress external interferences. In addition, the data
515 were corrected for head motion and downsampled to 250 Hz. The data were then converted
516 into Statistical Parametric Mapping (SPM)⁵¹ format and analyzed in MATLAB (MathWorks,
517 Natick, MA, USA) with the Oxford Centre for Human Brain Activity (OHBA) Software
518 Library (OSL) (<https://ohba-analysis.github.io/osl-docs/>), a freely available software that
519 builds upon Fieldtrip⁵², FSL⁵³, and SPM toolboxes. The signal was high-pass filtered (0.1
520 Hz of cutoff) to remove external frequencies and a notch filter was subsequently applied (48

521 – 52 Hz) to correct for inferences of the electric current. The signal was further downsampled
522 to 150 Hz and the continuous MEG data were visually inspected to remove artifacts using the
523 OSLview tool. An independent component analysis (ICA) was performed to remove EOG
524 and ECG components. After reconstructing the signal with the remaining components⁵⁴, the
525 data were epoched into 160 trials (80 excerpts from each musical piece). Each trial lasted
526 1350 ms (1250 ms plus 100 ms of baseline time) and further analyses were performed on
527 correctly identified trials only (see **Figure 1C**).

528 The raw MEG sensor data (204 planar gradiometers and 102 magnetometers) were first
529 preprocessed by MaxFilter⁵⁰ in order to suppress external interferences. In addition, the data
530 were corrected for head motion and downsampled to 250 Hz. The data were then converted
531 into Statistical Parametric Mapping (SPM)⁵¹ format and analyzed in MATLAB (MathWorks,
532 Natick, MA, USA) with the Oxford Centre for Human Brain Activity (OHBA) Software
533 Library (OSL) (<https://ohba-analysis.github.io/osl-docs/>), a freely available software that
534 builds upon Fieldtrip⁵², FSL⁵³, and SPM toolboxes. The signal was high-pass filtered (0.1
535 Hz of cutoff) to remove external frequencies and a notch filter was subsequently applied (48
536 – 52 Hz) to correct for inferences of the electric current. The signal was further downsampled
537 to 150 Hz and the continuous MEG data were visually inspected to remove artifacts using the
538 OSLview tool. An independent component analysis (ICA) was performed to remove EOG
539 and ECG components. After reconstructing the signal with the remaining components⁵⁴, the
540 data were epoched into 160 trials (80 excerpts from each musical piece). Each trial lasted
541 1350 ms (1250 ms plus 100 ms of baseline time) and further analyses were performed on
542 correctly identified trials only (see **Figure 1C**).

543

544 **MEG sensor data analysis**

545 The primary focus of this study was on detecting differences in the brain activity underlying
546 the recognition of tonal versus atonal musical sequences. However, the data were first
547 analyzed at the MEG sensor level to verify that the neural signal was stronger for memorized
548 versus novel musical sequences. This first step was essential to replicate previous findings
549 obtained using a very similar experimental setting and paradigm and thus assess the quality of
550 our data³⁸⁻⁴⁰.

551 Following the preprocessing of the neural data, and in accordance with MEG analysis
552 guidelines⁵⁵, all trials belonging to one condition were averaged together. This procedure
553 resulted in four mean trials: one for memorized trials and one for novel trials for each musical
554 piece (i.e., memorized tonal, novel tonal, memorized atonal, novel atonal). Next, each pair of

555 planar gradiometers was combined by a sum root square. Paired-samples t-tests ($\alpha = .01$)
556 were then calculated to contrast the memorized and novel conditions for both the tonal and
557 atonal pieces, independently. This was performed for each combined planar gradiometer and
558 each time-point in the time-range 0 – 2500 ms (from the onset of the first tone of the musical
559 sequences) in order to determine which condition generated a stronger neural signal. The
560 analyses were calculated for planar gradiometers, since these sensors are less affected by
561 external noise and thus highly reliable when computing analyses at the MEG sensor level⁵⁵⁻
562⁵⁸. Multiple comparisons were corrected using cluster-based Monte Carlo simulations (MCS)
563⁵⁹ ($\alpha = .001$, 1000 permutations) on the significant t-tests' results. Specifically, for each
564 timepoint, a 2D matrix was generated reproducing the spatial location of the MEG channels
565 and the results of the t-tests of each MEG channel binarized according to their p -values (0s
566 for not significant tests and 1s for significant tests [i.e., $p < .01$]). The elements of the
567 resulting 3D matrix were then submitted to 1000 permutations. For each permutation, we
568 identified the maximum cluster of permuted 1s, and we built a reference distribution using
569 the maximum cluster sizes detected for each of the 1000 permutations. Finally, the original
570 clusters that had a larger size than 99.9% of the maximum cluster sizes of the permuted data
571 were considered significant.

572

573 **Source reconstruction**

574 After examining the strength of the neural signals at the MEG sensor level, we focused on the
575 main aim of the study, which was to investigate the neural differences underlying the
576 recognition of tonal versus atonal musical sequences in MEG reconstructed source space. To
577 perform this analysis, we localized the brain sources of the neural signal recorded in the MEG
578 channels. This procedure required designing a forward model, computing the inverse
579 solution (in this case, using a beamforming approach), and identifying the statistically
580 significant brain sources underlying the recognition of tonal and atonal sequences and their
581 contrasts over time. **Figure 1D** shows the graphical depiction of the source reconstruction
582 analyses.

583

584 *Beamforming*

585 Before computing the source reconstruction algorithm, the continuous data were band-pass
586 filtered into two frequency bands: a slow band (delta, 0.1 – 1 Hz) and a fast band (theta, 2 – 8
587 Hz). These bands were selected based on the findings reported by Bonetti et al.³⁸⁻⁴⁰, which
588 suggested that the theta band was responsible for a sensorial elaboration of each object (tone)

589 of the sequence, while the delta band was implicated in the recognition of the holistic
590 temporal sequence. The filtered data were then epoched and the brain sources that generated
591 the signal were calculated.

592 First, an overlapping-spheres forward model was computed using an 8-mm grid. This
593 theoretical head model considers each brain source as an active dipole and describes how the
594 unitary strength of such a dipole is reflected across the MEG sensors⁶⁰. Using the
595 information collected with the 3D digitizer, the MEG data and individual T1-weighted
596 images were co-registered and the forward model was subsequently computed. An MNI152-
597 T1 template with 8-mm spatial resolution was used in four cases in which the individual
598 anatomical scans were not available. Second, a beamforming algorithm was employed as the
599 inverse model. This is one of the most widely used algorithms for estimating the brain
600 sources from MEG channels' data and consists of utilizing a different set of weights which
601 are sequentially applied to the source locations (dipoles) for isolating the contribution of each
602 source to the activity recorded by the MEG channels for each time-point^{55, 61, 62}.

603

604 *General Linear Model*

605 After estimating the brain sources of the signal recorded on the MEG channels, a General
606 Linear Model (GLM) was estimated sequentially for each timepoint at each dipole location.
607 At the first level, the main effect of memorized and novel conditions, as well as their contrast,
608 was computed independently for each participant. At the group level, t-tests were carried out
609 for each dipole location to obtain the main effect of tonal, atonal and their contrast computed
610 on all aggregated participants. The GLMs were estimated independently for both the tonal
611 and atonal data and for both frequency bands.

612

613 *Brain activity underlying the development of the musical sequences*

614 To determine the temporal evolution of the brain activity underlying musical sequences'
615 recognition, cluster-based MCS were estimated for five specific time-windows that
616 corresponded to each of the five tones comprising the musical sequences. This procedure was
617 carried out independently for both tonal and atonal data and for both frequency bands. Thus,
618 ten cluster-based MCS were calculated for each musical piece (five tones x two frequency
619 bands) on the results of the group-level analysis with an adjusted alpha level of .001 ($\alpha =$
620 $0.01/10 = .001$). This procedure allowed detecting the spatial clusters of significant brain
621 sources underlying the recognition of the tonal and atonal musical sequences. For each of the
622 MCSs, the data were sub-averaged in the time-window of interest (e.g., the time-window for

623 the first tone of the musical sequences) and then submitted to 1000 permutations to build a
624 reference distribution of the maximum cluster sizes detected in the permuted data. Then,
625 using the same procedure as with the MEG channels, the original cluster sizes were compared
626 to the reference distribution and were considered significant if their size was bigger than
627 99.9% of the maximum cluster sizes of the permuted data.

628 Importantly, further analyses were conducted to assess the differences between tonal and
629 atonal data when recognizing memorized trials for both the delta and theta frequency bands.
630 For each participant, a t-test ($\alpha = 0.01$) was computed for each source location and for the
631 five time-windows corresponding to each musical tone, contrasting the brain activity
632 underlying the recognition of tonal versus atonal music. Multiple comparisons were corrected
633 for by using cluster-based MCS, as described above. In this case, ten MCS ($\alpha = .001$, 1000
634 permutations) were calculated on the significant t-test results (five tones x two frequency
635 ranges).
636

637 **Data availability**

638 The code and anonymized neuroimaging data from the experiment will be made available
639 upon request. Regarding the data, we will be able to share it when it is completely
640 anonymized and cannot lead in any way to the original participants identity, according to
641 Danish regulations. Otherwise, a data sharing agreement must be made.

642 **References**

- 643 1. Gabrieli, J.D. Cognitive neuroscience of human memory. *Annual Review of Psychology*
644 **49**, 87-115; 10.1146/annurev.psych.49.1.87 (1998).
- 645 2. Daumas, S., Halley, H., Frances, B., & Lassalle, J.M. Encoding, consolidation, and
646 retrieval of contextual memory: differential involvement of dorsal CA3 and CA1
647 hippocampal subregions. *Learning and Memory* **12**, 375-82; 10.1101/lm.81905 (2005).
- 648 3. Greicius, M.D., Krasnow, B., Boyett-Anderson, J.M., Eliez, S., Schatzberg, A.F., Reiss,
649 A.L., & Menon, V. Regional analysis of hippocampal activation during memory
650 encoding and retrieval: fMRI study. *Hippocampus* **13**, 164-74; 10.1002/hipo.10064
651 (2003).
- 652 4. Meltzer, J.A., & Constable, R.T. Activation of human hippocampal formation reflects
653 success in both encoding and cued recall of paired associates. *NeuroImage* **24**, 384-97;
654 10.1016/j.neuroimage.2004.09.001 (2005).
- 655 5. Bird, C.M. The role of the hippocampus in recognition memory. *Cortex* **93**, 155-165;
656 10.1016/j.cortex.2017.05.016 (2017).
- 657 6. Eichenbaum, H., Yonelinas, A.P., & Ranganath, C. The medial temporal lobe and
658 recognition memory. *Annual Review of Neuroscience* **30**, 123-52;
659 10.1146/annurev.neuro.30.051606.094328 (2007).
- 660 7. Wiltgen, B.J., Brown, R.A., Talton, L.E., & Silva, A.J. New circuits for old memories:
661 the role of the neocortex in consolidation. *Neuron* **44**, 101-8;
662 10.1016/j.neuron.2004.09.015 (2004).
- 663 8. van Kesteren, M.T., Fernandez, G., Norris, D.G., & Hermans, E.J. Persistent schema-
664 dependent hippocampal-neocortical connectivity during memory encoding and
665 postencoding rest in humans. *Proceedings of the National Academy of Sciences of the*
666 *United States of America* **107**, 7550-5; 10.1073/pnas.0914892107 (2010).
- 667 9. Mehta, M.R. Cortico-hippocampal interaction during up-down states and memory
668 consolidation. *Nature Neuroscience* **10**, 13-5; 10.1038/nn0107-13 (2007).
- 669 10. Aggleton, J.P., & Brown, M.W. Interleaving brain systems for episodic and recognition
670 memory. *Trends in Cognitive Sciences* **10**, 455-63; 10.1016/j.tics.2006.08.003 (2006).
- 671 11. DiCarlo, J.J., Zoccolan, D., & Rust, N.C. How does the brain solve visual object
672 recognition? *Neuron* **73**, 415-34; 10.1016/j.neuron.2012.01.010 (2012).
- 673 12. Sato, W., & Yoshikawa, S. Recognition memory for faces and scenes. *Journal of*
674 *General Psychology* **140**, 1-15; 10.1080/00221309.2012.710275 (2013).

- 675 13. Dehaene, S., Meyniel, F., Wacongne, C., Wang, L., & Pallier, C. The Neural
676 Representation of Sequences: From Transition Probabilities to Algebraic Patterns and
677 Linguistic Trees. *Neuron* **88**, 2-19; 10.1016/j.neuron.2015.09.019 (2015).
- 678 14. Kang, H., Agus, T.R., & Pressnitzer, D. Auditory memory for random time patterns.
679 *Journal of the Acoustical Society of America* **142**, 2219; 10.1121/1.5007730 (2017).
- 680 15. Peretz, I., & Zatorre, R.J., *The cognitive neuroscience of music*. 2003: OUP Oxford.
- 681 16. Vuust, P., Ostergaard, L., Pallesen, K.J., Bailey, C., & Roepstorff, A. Predictive coding
682 of music--brain responses to rhythmic incongruity. *Cortex* **45**, 80-92;
683 10.1016/j.cortex.2008.05.014 (2009).
- 684 17. Vuust, P., Dietz, M.J., Witek, M., & Kringelbach, M.L. Now you hear it: a predictive
685 coding model for understanding rhythmic incongruity. *Annals of the New York
686 Academy of Sciences*, 10.1111/nyas.13622 (2018).
- 687 18. Vuust, P., Heggli, O.A., Friston, K.J., & Kringelbach, M.L. Music in the brain. *Nature
688 Reviews: Neuroscience*, 10.1038/s41583-022-00578-5 (2022).
- 689 19. Koelsch, S., Vuust, P., & Friston, K. Predictive Processes and the Peculiar Case of
690 Music. *Trends in Cognitive Sciences* **23**, 63-77; 10.1016/j.tics.2018.10.006 (2019).
- 691 20. Schroger, E., Marzecova, A., & SanMiguel, I. Attention and prediction in human
692 audition: a lesson from cognitive psychophysiology. *European Journal of Neuroscience*
693 **41**, 641-64; 10.1111/ejn.12816 (2015).
- 694 21. Rohrmeier, M.A., & Koelsch, S. Predictive information processing in music cognition.
695 A critical review. *International Journal of Psychophysiology* **83**, 164-75;
696 10.1016/j.ijpsycho.2011.12.010 (2012).
- 697 22. Quiroga-Martinez, D.R., Hansen, N.C., Hojlund, A., Pearce, M., Brattico, E., & Vuust,
698 P. Decomposing neural responses to melodic surprise in musicians and non-musicians:
699 Evidence for a hierarchy of predictions in the auditory system. *NeuroImage* **215**,
700 116816; 10.1016/j.neuroimage.2020.116816 (2020).
- 701 23. Quiroga-Martinez, D.R., Hansen, N.C., Hojlund, A., Pearce, M.T., Brattico, E., &
702 Vuust, P. Reduced prediction error responses in high-as compared to low-uncertainty
703 musical contexts. *Cortex* **120**, 181-200; 10.1016/j.cortex.2019.06.010 (2019).
- 704 24. Lumaca, M., Trusbak Haumann, N., Brattico, E., Grube, M., & Vuust, P. Weighting of
705 neural prediction error by rhythmic complexity: A predictive coding account using
706 mismatch negativity. *European Journal of Neuroscience* **49**, 1597-1609;
707 10.1111/ejn.14329 (2019).

- 708 25. Koelsch, S., Fritz, T., Schulze, K., Alsup, D., & Schlaug, G. Adults and children
709 processing music: an fMRI study. *NeuroImage* **25**, 1068-76;
710 10.1016/j.neuroimage.2004.12.050 (2005).
- 711 26. Putkinen, V., Tervaniemi, M., & Huotilainen, M. Musical playschool activities are
712 linked to faster auditory development during preschool-age: a longitudinal ERP study.
713 *Scientific Reports* **9**, 11310; 10.1038/s41598-019-47467-z (2019).
- 714 27. Pearce, M.T. Statistical learning and probabilistic prediction in music cognition:
715 mechanisms of stylistic enculturation. *Annals of the New York Academy of Sciences*,
716 10.1111/nyas.13654 (2018).
- 717 28. Witek, M.A., Clarke, E.F., Wallentin, M., Kringelbach, M.L., & Vuust, P. Syncopation,
718 body-movement and pleasure in groove music. *PloS One* **9**, e94446;
719 10.1371/journal.pone.0094446 (2014).
- 720 29. Matthews, T.E., Witek, M.A., Heggli, O.A., Penhune, V.B., & Vuust, P. The sensation
721 of groove is affected by the interaction of rhythmic and harmonic complexity. *PloS One*
722 **14**, e0204539; (2019).
- 723 30. Konvalinka, I., Vuust, P., Roepstorff, A., & Frith, C.D. Follow you, follow me:
724 continuous mutual prediction and adaptation in joint tapping. *Quarterly Journal of*
725 *Experimental Psychology (2006)* **63**, 2220-30; 10.1080/17470218.2010.497843 (2010).
- 726 31. Heggli, O.A., Konvalinka, I., Kringelbach, M.L., & Vuust, P. Musical interaction is
727 influenced by underlying predictive models and musical expertise. *Scientific Reports* **9**,
728 1-13; (2019).
- 729 32. Pecenka, N., & Keller, P.E. The role of temporal prediction abilities in interpersonal
730 sensorimotor synchronization. *Experimental Brain Research* **211**, 505-15;
731 10.1007/s00221-011-2616-0 (2011).
- 732 33. Vuust, P., & Kringelbach, M.L. The pleasure of making sense of music.
733 *Interdisciplinary science reviews* **35**, 166-182; (2010).
- 734 34. Gebauer, L., Kringelbach, M.L., & Vuust, P. Ever-changing cycles of musical pleasure:
735 The role of dopamine and anticipation. *Psychomusicology: Music, Mind, and Brain* **22**,
736 152; (2012).
- 737 35. Brattico, E., & Pearce, M. The neuroaesthetics of music. *Psychology of Aesthetics,*
738 *Creativity, and the Arts* **7**, 48; (2013).
- 739 36. Alluri, V., Toiviainen, P., Jaaskelainen, I.P., Glerean, E., Sams, M., & Brattico, E.
740 Large-scale brain networks emerge from dynamic processing of musical timbre, key
741 and rhythm. *NeuroImage* **59**, 3677-89; 10.1016/j.neuroimage.2011.11.019 (2012).

- 742 37. Burunat, I., Alluri, V., Toiviainen, P., Numminen, J., & Brattico, E. Dynamics of brain
743 activity underlying working memory for music in a naturalistic condition. *Cortex* **57**,
744 254-69; 10.1016/j.cortex.2014.04.012 (2014).
- 745 38. Bonetti, L., Brattico, E., Carlomagno, F., Cabral, J., Stevner, A., Deco, G., Whybrow,
746 P.C., Pearce, M., Pantazis, D., & Vuust, P. Spatiotemporal brain dynamics during
747 recognition of the music of Johann Sebastian Bach. *bioRxiv*, (2020).
- 748 39. Bonetti, L., Brattico, E., Bruzzone, S.E.P., Donati, G., Deco, G., Pantazis, D., Vuust, P.,
749 & Kringelbach, M.L. Temporal pattern recognition in the human brain: a dual
750 simultaneous processing. *bioRxiv*, (2021).
- 751 40. Bonetti, L., Brattico, E., Carlomagno, F., Donati, G., Cabral, J., Haumann, N.T., Deco,
752 G., Vuust, P., & Kringelbach, M.L. Rapid encoding of musical tones discovered in
753 whole-brain connectivity. *NeuroImage* **245**, 118735;
754 10.1016/j.neuroimage.2021.118735 (2021).
- 755 41. Serra, J., Corral, A., Boguna, M., Haro, M., & Arcos, J.L. Measuring the evolution of
756 contemporary western popular music. *Scientific Reports* **2**, 521; 10.1038/srep00521
757 (2012).
- 758 42. Mencke, I., Quiroga-Martinez, D.R., Omigie, D., Michalareas, G., Schwarzacher, F.,
759 Haumann, N.T., Vuust, P., & Brattico, E. Prediction under uncertainty: Dissociating
760 sensory from cognitive expectations in highly uncertain musical contexts. *Brain*
761 *Research* **1773**, 147664; 10.1016/j.brainres.2021.147664 (2021).
- 762 43. Vuvan, D.T., Podolak, O.M., & Schmuckler, M.A. Memory for musical tones: the
763 impact of tonality and the creation of false memories. *Frontiers in Psychology* **5**, 582;
764 10.3389/fpsyg.2014.00582 (2014).
- 765 44. Ockelford, A., & Sergeant, D. Musical expectancy in atonal contexts: Musicians’
766 perception of “antistructure”. *Psychology of Music* **41**, 139-174; (2013).
- 767 45. Mencke, I., Omigie, D., Wald-Fuhrmann, M., & Brattico, E. Atonal Music: Can
768 Uncertainty Lead to Pleasure? *Frontiers in Neuroscience* **12**, 979;
769 10.3389/fnins.2018.00979 (2018).
- 770 46. Daynes, H. Listeners’ perceptual and emotional responses to tonal and atonal music.
771 *Psychology of Music* **39**, 468-502; (2011).
- 772 47. Nieminen, S., Istók, E., Brattico, E., & Tervaniemi, M. The development of the
773 aesthetic experience of music: preference, emotions, and beauty. *Musicae Scientiae* **16**,
774 372-391; (2012).

- 775 48. Proverbio, A.M., Manfrin, L., Arcari, L.A., De Benedetto, F., Gazzola, M.,
776 Guardamagna, M., Lozano Nasi, V., & Zani, A. Non-expert listeners show decreased
777 heart rate and increased blood pressure (fear bradycardia) in response to atonal music.
778 *Frontiers in Psychology* **6**, 1646; 10.3389/fpsyg.2015.01646 (2015).
- 779 49. Krumhansl, C.L., & Cuddy, L.L., *A theory of tonal hierarchies in music*, in *Music*
780 *perception*. 2010, Springer. p. 51-87.
- 781 50. Taulu, S., & Simola, J. Spatiotemporal signal space separation method for rejecting
782 nearby interference in MEG measurements. *Physics in Medicine and Biology* **51**, 1759-
783 68; 10.1088/0031-9155/51/7/008 (2006).
- 784 51. Penny, W.D., Friston, K.J., Ashburner, J.T., Kiebel, S.J., & Nichols, T.E., *Statistical*
785 *parametric mapping: the analysis of functional brain images*. 2011: Elsevier.
- 786 52. Oostenveld, R., Fries, P., Maris, E., & Schoffelen, J.M. FieldTrip: Open source
787 software for advanced analysis of MEG, EEG, and invasive electrophysiological data.
788 *Computational Intelligence and Neuroscience* **2011**, 156869; 10.1155/2011/156869
789 (2011).
- 790 53. Woolrich, M.W., Jbabdi, S., Patenaude, B., Chappell, M., Makni, S., Behrens, T.,
791 Beckmann, C., Jenkinson, M., & Smith, S.M. Bayesian analysis of neuroimaging data
792 in FSL. *NeuroImage* **45**, S173-86; 10.1016/j.neuroimage.2008.10.055 (2009).
- 793 54. Mantini, D., Della Penna, S., Marzetti, L., de Pasquale, F., Pizzella, V., Corbetta, M., &
794 Romani, G.L. A signal-processing pipeline for magnetoencephalography resting-state
795 networks. *Brain Connectivity* **1**, 49-59; 10.1089/brain.2011.0001 (2011).
- 796 55. Gross, J., Baillet, S., Barnes, G.R., Henson, R.N., Hillebrand, A., Jensen, O., Jerbi, K.,
797 Litvak, V., Maess, B., Oostenveld, R., Parkkonen, L., Taylor, J.R., van Wassenhove,
798 V., Wibral, M., & Schoffelen, J.M. Good practice for conducting and reporting MEG
799 research. *NeuroImage* **65**, 349-63; 10.1016/j.neuroimage.2012.10.001 (2013).
- 800 56. Bonetti, L., Haumann, N.T., Vuust, P., Kliuchko, M., & Brattico, E. Risk of depression
801 enhances auditory Pitch discrimination in the brain as indexed by the mismatch
802 negativity. *Clinical Neurophysiology* **128**, 1923-1936; 10.1016/j.clinph.2017.07.004
803 (2017).
- 804 57. Bonetti, L., Haumann, N.T., Brattico, E., Kliuchko, M., Vuust, P., Sarkamo, T., &
805 Naatanen, R. Auditory sensory memory and working memory skills: Association
806 between frontal MMN and performance scores. *Brain Research* **1700**, 86-98;
807 10.1016/j.brainres.2018.06.034 (2018).

- 808 58. Bonetti, L., Bruzzone, S.E.P., Sedghi, N.A., Haumann, N.T., Paunio, T., Kantojarvi, K.,
809 Kliuchko, M., Vuust, P., & Brattico, E. Brain predictive coding processes are associated
810 to COMT gene Val158Met polymorphism. *NeuroImage* **233**, 117954;
811 10.1016/j.neuroimage.2021.117954 (2021).
- 812 59. Kroese, D.P., Taimre, T., & Botev, Z.I. Handbook of Monte Carlo Methods. John
813 Willey & Sons. Inc., Hoboken, New Jersey, (2011).
- 814 60. Huang, M.X., Mosher, J.C., & Leahy, R.M. A sensor-weighted overlapping-sphere
815 head model and exhaustive head model comparison for MEG. *Physics in Medicine and*
816 *Biology* **44**, 423-40; 10.1088/0031-9155/44/2/010 (1999).
- 817 61. Brookes, M.J., Stevenson, C.M., Barnes, G.R., Hillebrand, A., Simpson, M.I., Francis,
818 S.T., & Morris, P.G. Beamformer reconstruction of correlated sources using a modified
819 source model. *NeuroImage* **34**, 1454-65; 10.1016/j.neuroimage.2006.11.012 (2007).
- 820 62. Hillebrand, A., & Barnes, G.R. Beamformer analysis of MEG data. *International*
821 *Review of Neurobiology* **68**, 149-71; 10.1016/S0074-7742(05)68006-3 (2005).
- 822 63. Lewicki, M.S. Efficient coding of natural sounds. *Nature Neuroscience* **5**, 356-63;
823 10.1038/nn831 (2002).
- 824 64. Norman-Haignere, S.V., Kanwisher, N., McDermott, J.H., & Conway, B.R. Divergence
825 in the functional organization of human and macaque auditory cortex revealed by fMRI
826 responses to harmonic tones. *Nature Neuroscience* **22**, 1057-1060; 10.1038/s41593-
827 019-0410-7 (2019).
- 828 65. Hackett, T.A. Anatomic organization of the auditory cortex. *Handbook of Clinical*
829 *Neurology* **129**, 27-53; 10.1016/B978-0-444-62630-1.00002-0 (2015).
- 830 66. Mashour, G.A., Roelfsema, P., Changeux, J.-P., & Dehaene, S. Conscious processing
831 and the global neuronal workspace hypothesis. *Neuron* **105**, 776-798; (2020).
- 832 67. Dehaene, S., Kerszberg, M., & Changeux, J.-P. A neuronal model of a global
833 workspace in effortful cognitive tasks. *Proceedings of the national Academy of*
834 *Sciences* **95**, 14529-14534; (1998).
- 835 68. Dehaene, S., & Naccache, L. Towards a cognitive neuroscience of consciousness: basic
836 evidence and a workspace framework. *Cognition* **79**, 1-37; 10.1016/s0010-
837 0277(00)00123-2 (2001).
- 838 69. Dehaene, S., & Changeux, J.P. Experimental and theoretical approaches to conscious
839 processing. *Neuron* **70**, 200-27; 10.1016/j.neuron.2011.03.018 (2011).